A mathematical model and mesh-free numerical method for contact-line motion in lubrication theory

Lennon Ó Náraigh

School of Mathematics and Statistics, University College Dublin, Belfield, Dublin 4, Ireland

October 2024

THERMASMART
Thermal Management
of Microprocessors

**SFI Centre for Research Training
in Foundations of Data Science**

Introduction

- Fluid Mechanics talk, specifically about **multiphase flows**.

Introduction

- Fluid Mechanics talk, specifically about **multiphase flows**.
- In multiphase flows, contact-line motion refers to the motion of the triple point, which represents the intersection of the interface with a solid wall.

Introduction

- Fluid Mechanics talk, specifically about **multiphase flows**.
- In multiphase flows, contact-line motion refers to the motion of the triple point, which represents the intersection of the interface with a solid wall.
- This appears as a boundary condition in the equations of motion.

Introduction

- Fluid Mechanics talk, specifically about **multiphase flows**.
- In multiphase flows, contact-line motion refers to the motion of the triple point, which represents the intersection of the interface with a solid wall.
- This appears as a boundary condition in the equations of motion.
- Because the boundary condition is to be applied at the interface, it is difficult to model contact-line motion.

Introduction

- Fluid Mechanics talk, specifically about **multiphase flows**.
- In multiphase flows, contact-line motion refers to the motion of the triple point, which represents the intersection of the interface with a solid wall.
- This appears as a boundary condition in the equations of motion.
- Because the boundary condition is to be applied at the interface, it is difficult to model contact-line motion.
- Very loosely, this is the computational scientist's formulation of the **contact-line singularity problem**.

Aim of Talk
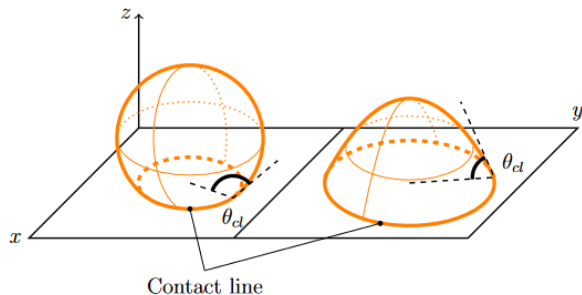
Liquid droplets on a horizontal surface. Image by KEP.

The aim of this talk is to provide an overview of the contact-line singularity problem:

- Present the overview from different perspectives;
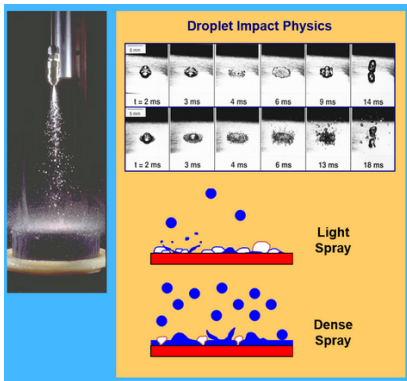- Present a novel regularization of the problem.

Motivation

Driver of research in CL motion: to produce accurate high-end multiphase simulations. Important for modelling a wide range of processes in industry (and nature). Also, **scientific curiosity**.

Hydrophilic plants – water repellent.
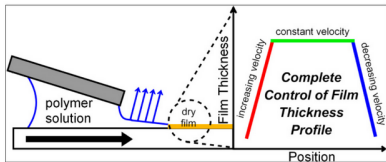
Thin-film coating

Spray cooling – droplet impact

Plan of talk

- High-level introduction to contact-line modelling in VOF and DIM
- The same, in the context of thin-film flows.
- Introduce novel regularization in the context of thin-film flows.

VOF – Review

The volume-of-fluid method for incompressible flows is a classic one-fluid formulation of the two-phase flow problem[1]. Instead of working with an indicator function,

$$\chi(\boldsymbol{x}) = \begin{cases} 1, & \text{if } \boldsymbol{x} \text{ is in phase 1,} \\ 0, & \text{if } \boldsymbol{x} \text{ is in phase 2,} \end{cases}$$

one works with a locally-averaged volume fraction:

$$\alpha(\boldsymbol{x}) = \frac{1}{V} \int_V \chi(\boldsymbol{x}) \mathrm{d}^3 x,$$

where V is a small test volume. Correspondingly,

$$\rho(\boldsymbol{x}) = \rho_1 \alpha(\boldsymbol{x}) + \rho_2 (1 - \alpha(\boldsymbol{x})),$$

and the same for the viscosity $\mu(\boldsymbol{x})$. Here, ρ_1 and ρ_2 are the constant densities of the individual phases.

---

[1] Brackbill, J.U., Kothe, D.B. and Zemach, C., 1992. A continuum method for modeling surface tension. *Journal of Computational Physics*, 100(2), pp.335-354.

VOF – Review

As the volume-averaging effectively smooths the interface between the phases, a continuous one-fluid equation of motion can be written down:

$$\rho(\boldsymbol{x}) \left(\frac{\partial \boldsymbol{u}}{\partial t} + \boldsymbol{u} \cdot \nabla \boldsymbol{u}\right) = -\nabla p + \nabla \cdot \left[\mu(\boldsymbol{x}) \left(\nabla \boldsymbol{u} + \nabla \boldsymbol{u}^T\right)\right] - \rho(\boldsymbol{x})g\mathbf{k} + \boldsymbol{F}_{ST}.$$

Conservation of mass (incl. incompressibility) require:

$$\frac{\partial \alpha}{\partial t} + \boldsymbol{u} \cdot \nabla \alpha = 0, \qquad \nabla \cdot \boldsymbol{u} = 0.$$

Here, $\boldsymbol{F}_{ST}$ is the surface-tension force. In the sharp-interface formulation, this would be:

$$\boldsymbol{F}_{ST} = \sigma \mathbf{n} \kappa \delta(\boldsymbol{x} - \boldsymbol{x}_I),$$

where σ is the surface tension, $\mathbf{n}$ is the unit normal to the interface, κ is the mean curvature, and $\boldsymbol{x}_I$ is the instantaneous interface location.

VOF – Review

The delta function is zero everywhere except at the interface location $\boldsymbol{x} = \boldsymbol{x}_I$. This can be re-written as $\delta(\boldsymbol{x} - \boldsymbol{x}_I) = |\nabla\alpha|\delta(\alpha - (1/2))$. Similarly,

$$\mathbf{n} = \left(\frac{\nabla\alpha}{|\nabla\alpha|}\right)_{\alpha=1/2}.$$

As the curvature is given by $\kappa = -\nabla \cdot \mathbf{n}$, this gives:

$$\boldsymbol{F}_{ST} = -\sigma\left[\nabla\alpha(\nabla \cdot \mathbf{n})\right]_{\alpha=1/2}.$$

The point of departure for the volume-of-fluid method is to distribute this force over the entire volume:

$$\boldsymbol{F}_{ST} \approx -\sigma\left[\nabla\alpha(\nabla \cdot \mathbf{n})\right],$$

This is a good approximation, because $\alpha \approx \text{Const} = 1$ or 0 away from the interface. Of course, the approximation does lead to the notorious **spurious currents**.

Boundary Conditions

If the contact line does not intersect the boundaries ($= \partial\Omega$) – the boundary condition on α is conservative: $\mathbf{n}_{\partial\Omega} \cdot \nabla\alpha = 0$ on $\partial\Omega$. Otherwise:

D. Boundary Conditions: Wall Adhesion

The effects of wall adhesion at fluid interfaces in contact with rigid boundaries in equilibrium can be estimated easily within the framework of the CSF model in terms of θ_{eq}, the equilibrium contact angle between the fluid and wall. The angle θ_{eq} is called the static contact angle because it is experimentally measured when the fluid is at rest. The equilibrium contact angle is not simply a material property of the fluid. It depends also on the smoothness and geometry of the wall [23].

The normal to the interface at points $\mathbf{x}_w$ on the wall is

$$\hat{n} = \hat{n}_{wall} \cos\theta_{eq} + \hat{n}_t \sin\theta_{eq}, \qquad (53)$$

where $\hat{n}_t$ lies in the wall and is normal to the contact line

between the interface and the wall at $\mathbf{x}_w$, and $\hat{n}_{wall}$ is the unit wall normal directed into the wall. The unit normal $\hat{n}_t$ is computed using (36) with the fluid color $\tilde{c}$ reflected at the wall.

Wall adhesion boundary conditions are more complex when the contact line is in motion, i.e., when the fluid in contact with the wall is moving relative to the wall [23]. The equilibrium wall adhesion boundary condition in (53) may have to be generalized by replacing θ_{eq} with a dynamic contact angle, θ_d, that depends on local fluid and wall conditions.

Implementations

- Numerical implementations of the VoF method are based on Brackbill's ideas. To move the contact line along, a slip velocity is required.
- A new boundary condition $u = \lambda(\partial u/\partial z)$ at $z = 0$. Navier slip length λ.
- Physically, the slip length is $O(\text{nm})$.
- Practically, it is not possible to implement this. So numerical studies[2] use either $\lambda = 0$ or $\lambda \propto \Delta$, where Δ is the grid spacing.
- A further model is required for the **contact-line motion**:

$$\theta(t) = f(\theta_e, U, ...).$$

- Here, U is the contact-line velocity – sometimes taken to be the tangential velocity in the cell nearest to the contact line (MAC grid).
- **Intrinsic grid dependence**

---

[2]Legendre, D. and Maglio, M., 2015. Comparison between numerical models for the simulation of moving contact lines. *Computers & Fluids*, 113, pp.2-13.

Implementations

This is the basic idea e.g. in the InterFoam contact-angle model, where $\theta(t) = \theta_e + (\theta_a - \theta_r) \tanh(U/U_\theta)$ is standard. Kistler's contact-angle model is more accurate.

E.g. Ref.[3]

2.1.2. Kistler's dynamic contact angle model

The empirical dynamic contact angle model developed by Kistler (1993) is based on Hoffman's empirical function (Hoffman, 1975). In this correlation the dynamic contact angle is dependent on the static contact angle and the contact line velocity through the Ca number. The model is valid for advancing contact lines and is given in the form

$$\theta_D = f_H \left(\text{Ca} + f_H^{-1}(\theta_E) \right), \tag{8}$$

where $f_H(x)$ is Hoffman's empirical function and $f_H^{-1}(x)$ is its inverse. Hoffman's empirical function is defined as

$$f_H(x) = \cos^{-1}\left(1 - 2\tanh\left(5.16\left(\frac{x}{1+1.31x^{0.99}} \right)^{0.706} \right) \right), \tag{9}$$

and the inverse of Hoffman's empirical function is closely approximated by the Hoffman-Voinov-Tanner law, Eq.(5), and has the form

$$f_H^{-1}(\theta_E) = \frac{\theta_E^3}{c_T}. \tag{10}$$

If experimental data of the contact angle hysteresis are available, the static contact angle, θ_E, in equations (8) and (10) is replaced by θ_A if the contact line is advancing. The final form of the model used for the advancing contact lines is

$$\theta_D = f_H \left(\text{Ca} + f_H^{-1}(\theta_A) \right). \tag{11}$$

---

[3]Göhl, J., Mark, A., Sasic, S. and Edelvik, F., 2018. An immersed boundary based dynamic contact angle framework for handling complex surfaces of mixed wettabilities. *International Journal of Multiphase Flow*, 109, pp.164–177.

Results – Droplet Impact
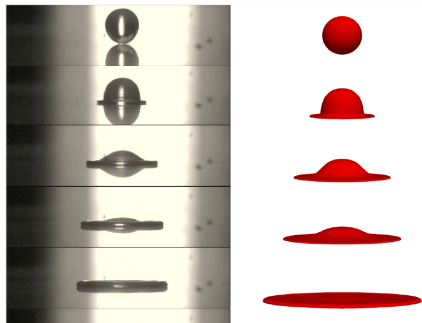
Droplet impact study. Left: high-speed camera. Right: OpenFOAM simulations. Parameters: $Re = 1700$ and $We = 20$. Image by Conor Quigley.

Version	Maximum Spreading [m]
Experiment	0.0180
Constant θ	0.0115
Dynamic θ	0.0140

TABLE I: Maximum spreading values.

DIM – Review

A phase-field function $C(\boldsymbol{x}, t)$ tracks which phase is occupied at position $\boldsymbol{x}$. Conventionally, $C = 1$ for liquid and $C = 0$ for gas, with $C = 0.5$ representing the interface.

The energy associated with interfaces is given by:

$$F[C] = \frac{\widehat{\sigma}}{\xi} \int \left[f_0(C) + \tfrac{1}{2}\xi^2 |\nabla C|^2 \right] \mathrm{d}^3 x,$$

where:

- $f_0(C)$ penalizes mixing (promotes creation of separate phases);
- $(1/2)\xi^2 |\nabla C|^2$ penalizes sharp gradients (diffuse interface);
- $\widehat{\sigma}$ related to the surface tension;
- ξ is a small lengthscale (interface thickness).

DIM – Review

A 'gradient-energy formulation' gives:

$$\frac{\partial C}{\partial t} + \boldsymbol{u} \cdot \nabla C = \nabla \cdot \left[M(C) \nabla \Phi \right],$$

where $M(C) \geq 0$ is the mobility and $\Phi = \delta F / \delta C$.

Again, we have a one-fluid formulation, so $\boldsymbol{u}$ is the velocity of the mixture, and $\rho(\boldsymbol{x}) = \rho_1 C + \rho_2 (1 - C)$, and similarly for the viscosity.

The 'Gradient-energy formulation' ensures that the energy is dissipated:

$$\frac{\mathrm{d}}{\mathrm{d}t} \left[\tfrac{1}{2} \int \rho \boldsymbol{u}^2 \mathrm{d}^3 x + F[C] \right] \leq 0.$$

DIM – Momentum Equation

The one-fluid momentum equation can be written as:

$$\rho(\boldsymbol{x})\left(\frac{\partial \boldsymbol{u}}{\partial t} + \boldsymbol{u} \cdot \nabla \boldsymbol{u}\right) = -\nabla p + \nabla \cdot \left[\mu(\boldsymbol{x})\left(\nabla \boldsymbol{u} + \nabla \boldsymbol{u}^T\right)\right] - \rho(\boldsymbol{x})g\mathbf{k} + \boldsymbol{F}_{ST}.$$

In the DIM context, the surface-tension force has the form:

$$\boldsymbol{F}_{ST} = \Phi \nabla C,$$

The sharp-interface formulation can be recovered in the limit as $\xi \to 0$.[4]

---

[4] Jacqmin, D., 1999. Calculation of two-phase Navier–Stokes flows using phase-field modeling. Journal of computational physics, 155(1), pp.96-127.

Boundary Conditions

- No-slip boundary conditions on velocity.
- Conservation of mass requires $\mathbf{n}_{\partial\Omega} \cdot \nabla\Phi = 0$ on $\partial\Omega$.
- The contact line moves through interfacial diffusion (diffuse-interface method).
- Since C-equation is 4th order, another BC is required.

Energy Formulation:

$$F = \frac{\widehat{\sigma}}{\xi} \int_{\Omega} \left[f_0(C) + \tfrac{1}{2}\xi^2 |\nabla C|^2 \right] \mathrm{d}\Omega + \int_{\partial\Omega} F_w(C) \mathrm{d}S,$$

where $F_w(C) \propto (\widehat{\sigma} \cos\theta_{eq})C$. Energy dissipation (bulk only) then requires:

$$\widehat{\sigma}\xi \left(\mathbf{n}_{\partial\Omega} \cdot \nabla C \right) = -F_w'(C).$$

Geometric Boundary Condition

An alternative formulation of the BC is the **geometric** one:

$$\mathbf{n}_{\partial\Omega} \cdot \nabla C = -\tan\left(\tfrac{1}{2}\pi - \theta_{eq}\right)$$
$$\times \left| \nabla C - (\mathbf{n}_{\partial\Omega} \cdot \nabla C)\,\mathbf{n}_{\partial\Omega} \right|.$$

Here, θ_{eq} is the equilibrium ('microscale') CA.

Implementation on 2D MAC grid:

$$C_{i,0} = C_{i,2}$$
$$+ \tan\left(\tfrac{1}{2}\pi - \theta_{eq}\right) \left| C_{i+1,1} - C_{i-1,1} \right|.$$

Subtle difference between the two approaches ——————→

Energy method: $\mathbf{n} \cdot \nabla C = -\cos\theta_s |\mathbf{t} \cdot \nabla C| / \sin\theta_s,$ (27)

while the surface-energy formulation of the wetting condition results in

Geometric method: $\mathbf{n} \cdot \nabla C = -\cos\theta_s |\mathbf{t} \cdot \nabla C| / \sin\theta_d$ (28)

by substituting $|\nabla C| = \mathbf{t} \cdot \nabla C / \sin\theta_d$ into Eq. (26). We can see that the microscale contact angle can be reproduced from the local distribution of C after the implementation of Eq. (27). However, this is not the case when using Eq. (28). In fact, the boundary condition (28) is comparable to imposing an effective contact angle θ, where $\min(\theta_s, \theta_d) \le \theta \le \max(\theta_s, \theta_d)$, instead of the microscale contact angle. Tracing back the difference between the two conditions, the cause is seen to be the fact that in Eq. (25) only the tangential component of ∇C appears on the right-hand side, whereas all components of ∇C are present on the right-hand side of Eq. (26). The application of either boundary condition will in fact change the normal component $\mathbf{n} \cdot \nabla C$, which will therefore affect the right-hand side of the latter, but not the former.

Results

Realistic parameter values for mm scale droplet:

	Water (L)	Air (G)
Dynamic Viscosity (μ)	$8.9 \times 10^{-4}\,\mathrm{Pa\,s}$	$1.837 \times 10^{-5}\,\mathrm{Pa\,s}$
Density (ρ)	$1000\,\mathrm{kg\,m^{-3}}$	$1.225\,\mathrm{kg\,m^{-3}}$

Droplet Radius (R_0)	$3\,\mathrm{mm}$
Surface Tension (σ)	$0.072\,\mathrm{N\,m^{-1}}$

Ref.[5]

---

[5] Ó Náraigh L. and Mairal, J., 2023. Analysis of the spreading radius in droplet impact: The two-dimensional case. Physics of Fluids, 35(10).

Results

Realistic parameter values for mm scale droplet:

	Water (L)	Air (G)
Dynamic Viscosity (μ)	$8.9 \times 10^{-4}\,\text{Pa}\,\text{s}$	$1.837 \times 10^{-5}\,\text{Pa}\,\text{s}$
Density (ρ)	$1000\,\text{kg}\,\text{m}^{-3}$	$1.225\,\text{kg}\,\text{m}^{-3}$

Droplet Radius (R_0)	$3\,\text{mm}$
Surface Tension (σ)	$0.072\,\text{N}\,\text{m}^{-1}$

Bond Number scaling: timescale $T_0 = R_0/U_0$, $U_0 = \sqrt{gR_0}$, hence strength of surface tension is $1/\text{Bo}$:

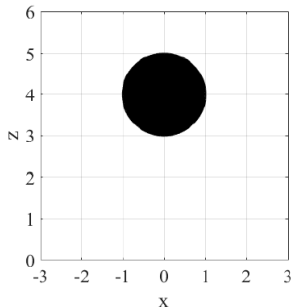$$\text{Bo} = \frac{\rho_L g R_0^2}{\sigma} = 1.226.$$

Also,

$$\text{Re} = \frac{\rho_L R_0 U_0}{\mu_L} = 578.0.$$

Ref.[5]

---

[5]Ó Náraigh L. and Mairal, J., 2023. Analysis of the spreading radius in droplet impact: The two-dimensional case. Physics of Fluids, 35(10).

Results

Realistic parameter values for mm scale droplet:

	Water (L)	Air (G)
Dynamic Viscosity (μ)	$8.9 \times 10^{-4}\,\mathrm{Pa\,s}$	$1.837 \times 10^{-5}\,\mathrm{Pa\,s}$
Density (ρ)	$1000\,\mathrm{kg\,m^{-3}}$	$1.225\,\mathrm{kg\,m^{-3}}$

Droplet Radius (R_0)	$3\,\mathrm{mm}$
Surface Tension (σ)	$0.072\,\mathrm{N\,m^{-1}}$

Droplet released from a height:

Bond Number scaling: timescale $T_0 = R_0/U_0$, $U_0 = \sqrt{gR_0}$, hence strength of surface tension is $1/\mathrm{Bo}$:

$$\mathrm{Bo} = \frac{\rho_L g R_0^2}{\sigma} = 1.226.$$

Also,

$$\mathrm{Re} = \frac{\rho_L R_0 U_0}{\mu_L} = 578.0.$$

Ref.[5]

---

[5]Ó Náraigh L. and Mairal, J., 2023. Analysis of the spreading radius in droplet impact: The two-dimensional case. Physics of Fluids, 35(10).

Results
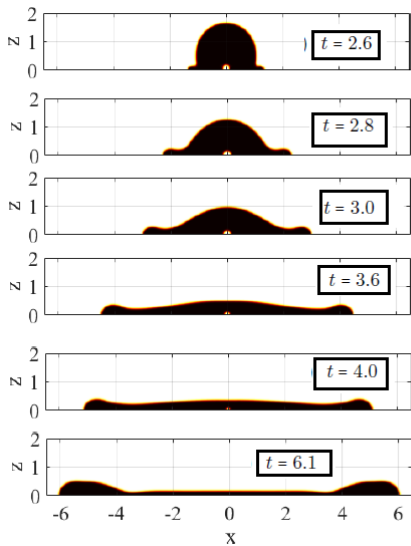
Energy budget:

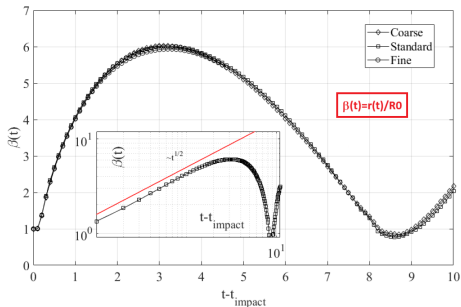$$E_{init} = E_{final} + \Delta E,$$
$$\Delta E = \text{Energy loss due to dissipation}$$
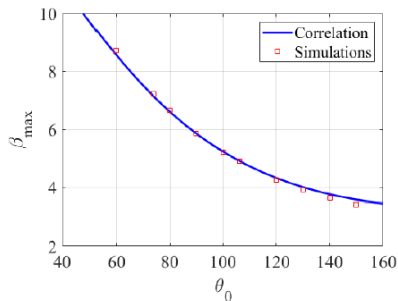
Dependence of β_{max} on the static contact angle for fixed Bo and Re. Squares: Simulations. Solid line: correlation

Small parameters

- Small parameters ξ and M (constant mobility).
- Take $\mathrm{Cn}, M \propto \Delta$.
- Establish grid convergence.
- Movement of CL via diffuse interface.

N	Δt	Δx	Cn	**M**	Label
161	10^{-4}	0.0375	$(4/3)\Delta x$	Δx	Coarse
321	10^{-4}	0.01875	—"—	—"—	Standard
641	$10^{-4}/2$	0.009375	—"—	—"—	Fine

Novel regularization

- Methods so far – CL slip on grid scale.
- Methods depend explicitly on grid scale but final results do not.
- Would like to introduce a more satisfactory method.
- Address the topic analytically first, in the context of **thin-film flows**.

Thil-Film Flows: Context
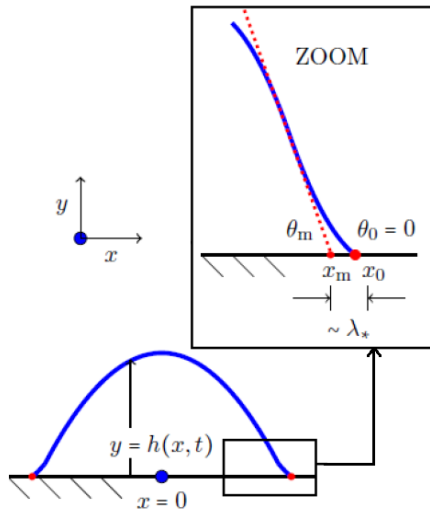
Thin film / Stokes Flow for $h(x,t)$:

$$\frac{\partial h}{\partial t} = -\frac{\partial}{\partial x}\left(h^n \frac{\partial^3 h}{\partial x^3}\right), \, x \in (-\infty, \infty).$$

Initial condition:

$$h(x, t=0) = h_0(x), \, h_0(x) \geq 0.$$

Boundary conditions: chosen for $|x| \to \infty$ such that equation conserves mass:

$$\frac{\mathrm{d}M}{\mathrm{d}t} = 0, \qquad M = \int_{-\infty}^{\infty} h(x,t)\mathrm{d}x.$$

The value $n = 3$ is physical – droplet spreading on a hydrophilic surface, no equilibrium contact angle.

Spreading Solution

Similarity solution:

$$h(x,t) = t^a f(x/t^a), \qquad a = \frac{1}{n+4}.$$

Substitute into $h_t = \partial_x(\cdots)$, obtain ordinary differential equation

$$f^n f''' = \frac{nf}{n+4}.$$

- Smooth solutions with compact support for $n < 3$.
- Point where solution touches down smoothly to zero is microscopic contact line.
- Microscopic contact line x_{cl} behaves as $x_{\mathrm{cl}} \sim t^{1/(n+4)}$.

Description breaks down at physically relevant value of $n = 3$. The analyst's view on the **contact-line singularity problem**.

Thin-Film Flows: Classical Regularizations

1. Navier Slip model – regularizes free-surface profile but not higher derivatives – hence, stress singularity remains.
2. Precursor Film model – requires ultra-thin precursor film; spreading droplets sits on top of this precursor layer. Ultra-thin precursor film has to extend indefinitely beyond the radius of the spreading droplet.

Novel Regularization

A novel regularization of the thin-film equation in the spirit of the diffuse-interface method has been introduced.[6] We work with $h(x,t)$ and also, a 'fuzzy' free-surface height,

$$\overline{h}(x,t) = \int_{-\infty}^{\infty} K(x-y;\alpha)h(y,t)\mathrm{d}y := K * h,$$

where $K(s;\alpha)$ is a smoothing kernel.

1. New method has continuous pressure profile (compare with Navier Slip model).

2. New method effectively has a precursor film which decays exponentially fast away from droplet core (decay rate α).

---

[6]Holm, D.D., Ó Náraigh, L. and Tronci, C., 2020. A geometric diffuse-interface method for droplet spreading. Proceedings of the Royal Society A, 476(2233), p.20190222.

Small length scales

Table: Summary of the various small length scales used in the different regularization methods

Method	Lengthscale
Navier Slip Model	Slip length
Attractive / Repulsive Potential	Precursor-film thickness
Diffuse-Interface Method	Diffuse-interface thickness
New Method	Length scale of smoothing kernel – **uncertainty** – *cf.* LES

Novel Regularization – the idea I

If we define

$$E = \tfrac{1}{2} \int_{-\infty}^{\infty} |\partial_x h|^2 \mathrm{d}x, \qquad \delta E/\delta h = -\partial_{xx} h \tag{1}$$

then the basic thin-film equation can be written as

$$\frac{\partial h}{\partial t} = \frac{\partial}{\partial x}\left[h\mu(h)\frac{\partial}{\partial x}\frac{\delta E}{\delta h} \right], \qquad \mu(h) = h^2. \tag{2}$$

By multiplying both sides of Equation (2) by $\delta E/\delta h$ and integrating , one obtains

$$\frac{\mathrm{d}E}{\mathrm{d}t} = -\int_{-\infty}^{\infty} h\mu(h)|\partial_{xx}h|^2 \mathrm{d}x \leq 0. \tag{3}$$

Novel Regularization – the idea II

If instead we define

$$\bar{E} = \tfrac{1}{2} \int_{-\infty}^{\infty} (\partial_x \overline{h})(\partial_x h) \mathrm{d}x, \tag{4}$$

where $\overline{h}$ is the fuzzy free-surface height, then

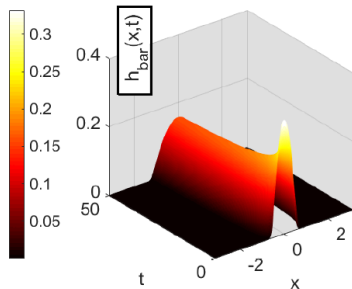$$\frac{\delta \bar{E}}{\delta h} = -\partial_{xx} \overline{h},$$

so that the evolution equation which minimizes the energy becomes

$$\partial_t h = -\partial_x \left[h\overline{\mu}(h, \overline{h}) \partial_x \partial_{xx} \overline{h} \right], \tag{5}$$

where we have defined $\overline{\mu}(h, \overline{h})$ so that the mobility depends in general on both h and $\overline{h}$ – in practice we will take $\overline{\mu} = \overline{h}^2$.
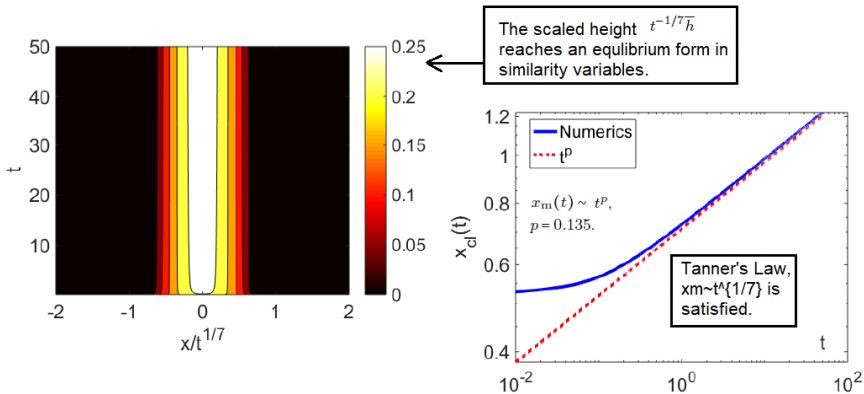
We then use $K = (1 - \alpha^2 \partial_{xx})^{-2}$.

Results I
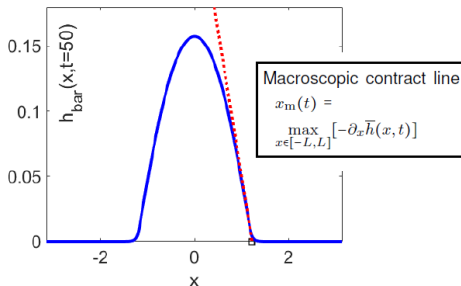
(a) Spacetime diagram showing the evolution of the diffuse surface height $\overline{h}(x,t)$. (b) Snapshot of the free-surface height $\overline{h}(x,t)$ at $t = 50$. The snapshot also shows the location of the macroscopic contract line x_{m}. Model parameter: $\alpha = 0.05$. Numerical parameters: $L = 2\pi$, $N = 500$ gridpoints, $\Delta t = 10^{-2}$.
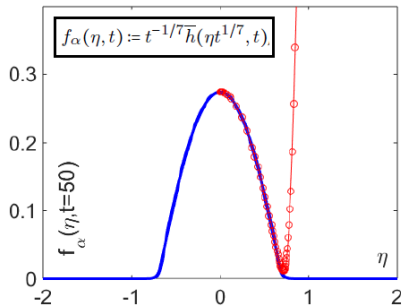
Ref.[7]

---

[7]Holm, D.D., Ó Náraigh, L. and Tronci, C., 2020. A geometric diffuse-interface method for droplet spreading. Proceedings of the Royal Society A, 476(2233), p.20190222.

Results II

The scaled height $t^{-1/7}\bar{h}$ reaches an equlibrium form in similarity variables.

$x_m(t) \sim t^p,$
$p = 0.135.$

Numerics
t^p

$x_{cl}(t)$

Tanner's Law, xm~t^{1/7} is satisfied.

Results III

Outer Solution

$$f_\alpha(\eta,t) := t^{-1/7}\overline{h}(\eta t^{1/7}, t)$$

— Numerical solution of regularized problem in similarity variables

—○— Solution of unregularized problem $f^2 f''' = \eta f/7$. showing blowup at contact line.

Inner solution with exponential decay in tails
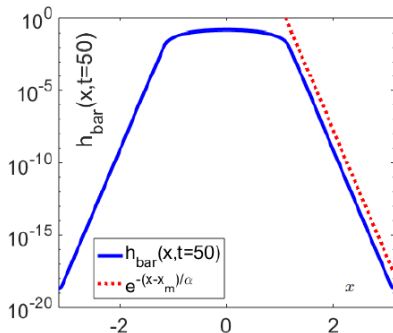
Plot of $\overline{h}(x, t = 50)$ showing the spatial structure of the solution in the tail, for $|x| \gg x_m$.

Inner and outer solutions match:

$$\overline{h}(x,t) \sim \begin{cases} t^{-1/7} f(x/t^{1/7}), & x \ll x_m(t), \\ A(t)e^{-|x-x_m(t)|/\alpha}, & |x| \gg x_m(t), \end{cases}$$

... hence, Tanner's Law is recovered.

Particle Solutions – Same idea as Camassa–Holm Equation

An intriguing aspect of the regularized set of equations is that it allows for weak solutions, which we call particle solutions:

$$h(x, t = 0) = \sum_{i=1}^{N} w_i \delta(x - x_i^0), \qquad h(x, t) = \sum_{i=1}^{N} \delta(x - x_i(t)),$$

where the $w_i's$ are positive weights, and the x_i's are 'particle trajectories', satisfying:

$$\frac{\mathrm{d}x_i}{\mathrm{d}t} = V_i, \qquad t > 0, \qquad x_i(0) = x_i^0,$$

and where the velocities V_i are obtained from the regularized PDE:

$$V_i = \left[\overline{h}(x_i, t)\right]^2 \left[\sum_{j=1}^{N} w_j K'''(x_i - x_j)\right],$$

and finally,

$$\overline{h}(x, t) = \sum_{j=1}^{N} w_j K(x - x_j).$$
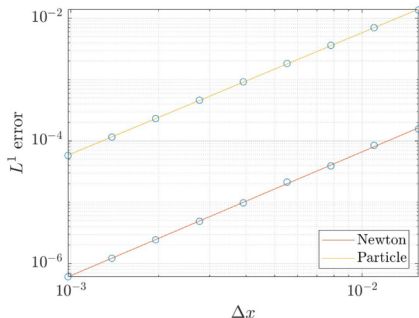
Convergence of Particle Solutions

- $\overline{h}$ is the exact solution.
- $\overline{h}_{\Delta x}$ is the numerical solution.
- Δx is the grid size (FD) or $N = 2L/\Delta x$ (particles).
- Assume:

$$\|\overline{h} - \overline{h}_{\Delta} x\|_{L^1} = C\Delta x^p + O(\Delta x^{p+1}).$$

- Let $\epsilon(\Delta x) = \|\overline{h}_{\Delta x} - \overline{h}_{\Delta x/2}\|_{L^1}$.
- Triangle inequality:

$$\epsilon(\Delta x) \le C\Delta x^p \left(1 - 1/2^p\right) + O(\Delta x^{p+1}).$$

Ref.[8]

Convergence plot of the finite-difference method and the particle method for the partial wetting case. Both lines have a slope of 2.0 on the log-log plot.

[8]Pang, K.E. and Ó Náraigh, L., 2022. A mathematical model and mesh-free numerical method for contact-line motion in lubrication theory. Environmental Fluid Mechanics, 22(2), pp.301-336.

Particles move around and concentrate in regions of high-curvature

- While FD method and PM are both $O(\Delta x^2)$, the pre-factor for the FD method is smaller.

- Prefactor C_{FD} and C_{PM}, with

$$C_{FD} < C_{PM}.$$

- However, the execution time of the PM is much faster.

- TLDR: The prefactor is not great but the Particle Method is Faster

- Crucially, **the particles move around and concentrate in regions of high-curvature**.

- Gives a mesh-free method which nevertheless mimics AMR.
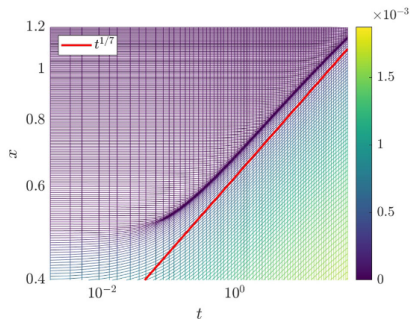
Evolution of the particle trajectories $x_i(t)$ (logarithmic scales on both axes). The colors indicate the weight corresponding to each particle w_i. The line $t^{1/7}$ is imposed to show that the trajectories follow a power law at late time

Partial Wetting

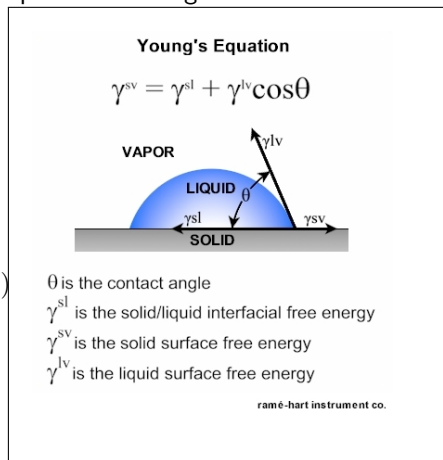Partial wetting – spreading goes on until equilibrium configuration is attained.

Force balance at equilibrium gives:

$$\cos\theta_{eq} = \frac{\gamma_{sv} - \gamma_{sl}}{\gamma_{lv}}.$$

Energy in thin-film formulation becomes:

$$E = \tfrac{1}{2}\gamma_{lv}\int_{-r}^{r} h_x^2 \mathrm{d}x + 2r\gamma_{lv}\left(1 - \cos\theta_{eq}\right)$$
$$+ \text{Constant}.$$

Droplet footprint (2D) is $2r$.

Young's Equation

$$\gamma^{sv} = \gamma^{sl} + \gamma^{lv}\cos\theta$$

VAPOR

LIQUID

γsl   γsv
SOLID

θ is the contact angle
γ^{sl} is the solid/liquid interfacial free energy
γ^{sv} is the solid surface free energy
γ^{lv} is the liquid surface free energy

ramé-hart instrument co.

Regularized Equation

As before, we regularize the contact-line motion. We take the surface energy term to be

$$\tfrac{1}{2}\gamma_{lv}\int_{-\infty}^{\infty}\overline{h}_x h_x \,\mathrm{d}x,$$

where $\overline{h}$ vanishes rapidly as $|x|\to\infty$.

We approximate the droplet footprint as

$$2r \propto \frac{A_0^2}{\langle h,\overline{h}\rangle}, \qquad \text{Const. is } \widehat{c},$$

where $A_0 = \int_{-\infty}^{\infty} h\,\mathrm{d}x = \int_{-\infty}^{\infty}\overline{h}\,\mathrm{d}x$.

Justification: If

$$h = \max\{0, 3A_0/(4r)[1-(x/r)^2]\},$$

then

$$\frac{A_0^2}{\langle h,\overline{h}\rangle} = \tfrac{5}{6}(2r) + O(\alpha^2).$$

Regularized TFE becomes:

$$\frac{\partial h}{\partial t} + \frac{\partial}{\partial x}\left(\mathcal{V}h\right) = 0,$$

$$\mathcal{V} = -\overline{h}^2 \frac{\partial}{\partial x}\frac{\delta \overline{E}}{\delta h}.$$

Results – Partial Wetting

Exact analytical solution at **equilibrium**:

$$\overline{h} = \begin{cases} B_1 \cos(\xi x) + B_2, & |x| < r, \\ C_1 \mathrm{e}^{-|x|/\alpha} + C_2 |x| \mathrm{e}^{-|x|/\alpha}, & |x| > r \end{cases}$$

Parameter:

$$\xi = \frac{2\widehat{c}(1 - \cos\theta_{eq})}{\langle h, \overline{h} \rangle^2}.$$

Matching conditions at $|x| = r$. Continuity of $\overline{h}$, $\overline{h}_x$, $\overline{h}_{xx}$. Also, $\int \overline{h} \, \mathrm{d}x = 1$.

Good **transient** results as well showing close agreement with the Cox–Voinov model:

$$\underbrace{\left(\frac{\partial h}{\partial x}\right)^3 \Big|_{x_m}}_{\approx [\theta(t)]^3} = \theta_{eq}^3$$

$$+ \, c \frac{\mathrm{d}x_m}{\mathrm{d}t} \log(x_m/d),$$

where c and d are fitting constants.

Reduces to Tanner's Law $x_m(t) \sim t^{1/7}$ when $\theta_{eq} = 0$.

Results and Discussion
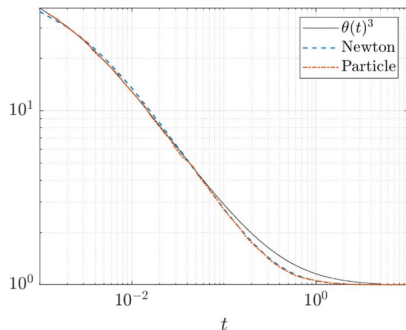
Plot of $[\theta(t)]^3$ (solid line) and $1 + c\dot{x}_{cl}\log(x_{cl}/d)$ (dashed and dot-dashed) as a function of time showing the agreement between GDIM and the Cox–Voinov theory for droplet spreading in the case of partial wetting.

- Still not sure about this approach:
  - ▶ Functional form for droplet-footprint size looks strange.
  - ▶ Equilibrium solution is complicated ('parabolic cap'?)
- Hence, while the regularization in case of complete wetting is hereby solved in a satisfactory way, the partial-wetting case remains something of a puzzle.

Conclusions

- Summarized modelling approach to CL problem in VOF and DIM.
- Parameters are explicitly dependent on grid size but final results are not.
- A little unsatisfactory, so alternative approaches are welcome.

Final words

- Introduced novel CL regularization in context of thin-film flows.
- Model uses 'fuzzy' $\overline{h}$ representing uncertainty in CL location, on a lengthscale α.
- Describes droplet spreading in the complete-wetting case.
- Still a little unsatisfactory in case of partial wetting.
- Also, would like to extend concept beyond thin-film flows.
- Discussion welcome.

Acknowledgments

People:

- Collaborators: Darryl Holm, Richard Smith, Cesare Tronci
- PhD student: Khang Ee Pang; MSc student: Juan Mairal
- Final-year BSc students (OpenFoam simulations, high-speed video analysis): Conor Quigley and Joseph Anderson

Funders: